Electronic Supporting Information

Efficient CO_2 hydrogenation to formate with iridium catalyst supported by porous organic polymer containing *N*-phenylpicolinamide motif

Yang Ding,[a,b] Yikang Duan,[a] Yang Li,[a,b] Jiasheng Wang,[a,b] Ming Bao,[a,b] Yuichiro Himeda [c] and Wan-Hui Wang *[a,b]

Centent

1. Characterization methods

All manipulations were carried out under a nitrogen atmosphere using standard Schlenk techniques or in a glovebox. All aqueous solutions were degassed before use. The XRD patterns of samples were taken on an XRD-7000S/L diffractometer in the 2θ range of 2°~40° at a scanning speed of 5 °/min using Al-Kα radiation (λ = 1.542 nm) at ambient temperature. The EA was detected using Vario EL cube instrument. A Renishaw inVia Raman spectrometer equipped with a He-Ne laser excitation source operating at 633 nm, was used for the collection of Raman spectra. The sample was pressed into a KBr-diluted self-supported wafer and placed into the sample holder. The spectrum region was recorded from 400 to 4000 cm^{-1} by averaging 32 scans with a resolution of 4 cm^{-1}. Nitrogen adsorption-desorption isotherms were carried out at 77 K on a JWBK300 Analyzer instrument. The specific surface area was calculated by the Brunauer-Emmett-Teller (BET) method. Before the measurements, the samples were degassed at 200°C under a vacuum for 2 h to remove physically adsorbed impurities. TGA was conducted on a thermal analysis system (TGA-1150, Shanghai Jiubin Instrument Co. Ltd.) under a flow of air with a heating rate of 10 °C/min from 25 to 1000 °C. SEM images were analyzed by using a Nova Nano SEM 450 system electron microscope. All samples were treated with gold coating before the test. XPS spectra were detected on an ESCALAB™ 250Xi system with Al Kα radiation as the excitation source. The software Avantage was employed to fit the peaks. The actual Ir loading of the samples was confirmed by Inductively coupled plasma mass spectrometry (ICP-MS, Agilent 7900X, Japan). FTIR spectra of the samples were recorded in the range of 45~4000 cm^{-1} on a Nicolet in10 MX & iS10 spectrophotometer. HPLC analysis was performed using Shimadzu LC-16 liquid chromatography. The mobile phase is 0.1% aqueous phosphoric acid solution, and the column is a TSKgel SCX-type column. The flow rate was 0.8 mL/min; column temperature: 40 ℃; injection volume: 20 μL; run time: 10 min. TEM, STEM, and EDS measurements made use of a Tecnai G2F30 STWIN operating at an accelerating voltage of 200 kV. ^{1}H NMR spectra were recorded on an AV III 500 HD 500 MHz spectrometer. Solid-state ^{13}C NMR (CP-MAS) spectroscopy was performed on Agilent DD2 Proton freq: 500 MHz instruments. CO_2-TPD (temperature-programmed desorption of CO_2) analysis was done on Autosorb-IQ-C from Quantachrome Corp.

2. Synthesis of POP supports and Ir catalysts.

2.1 Synthesis of POP-1 and Ir@POP-1(Cat-1)

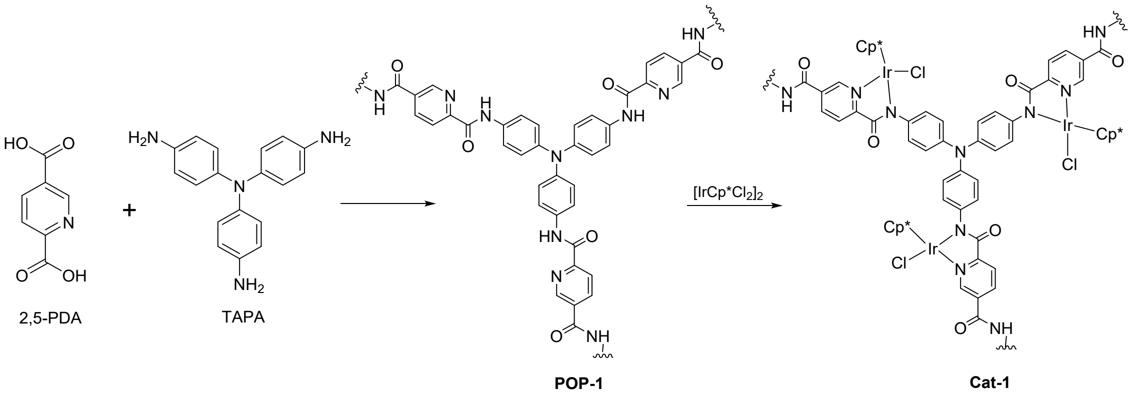

Fig. S1 Synthesis of **POP-1** and **Cat-1**.

2,5-PDA (0.8 mmol, 133.70 mg) was dispersed in anhydrous DMAc (4 mL) to obtain solution A. TAPA (0.4 mmol, 116.14 mg), LiCl (2 mmol, 84.78 mg), TPP (2 mmol, 620.56 mg), Et_3N (2 mmol, 202.38 mg) and DMAc (4 mL) were added into a 25 mL Schlenk flask to obtain solution B. Solution B was degassed and purged with argon (Ar) and heated to 140 °C with continuous stirring at 300 rpm. Then, the solution A was added to solution B. The mixture was maintained 140 °C for 3 days under an Ar atmosphere with continuous stirring at 300 rpm. After the reaction, the contents were allowed to cool naturally. The Ar was stopped and the final opaque solution was poured into methanol. The precipitate was then separated by filtration and washed several times with excess methanol and ultrapure water. The sample was dried under vacuum at 80 °C for 22 h to obtain the final product **POP-1** (160 mg). **POP-1** (40 mg) was dispersed in methanol (5 mL) by sonication. Subsequently, the desired $[Cp^*IrCl_2]_2$ was added to the aforementioned suspension and subjected to sonication for 10 min. After sonication, the mixture was stirred at 65 °C under reflux for 24 h and cooled. The solids were filtered, washed with an excess of methanol and dried under vacuum at 80 °C overnight to obtain catalyst **Cat-1**.

2.2 Synthesis of POP-2 and Ir@POP-2(Cat-2)

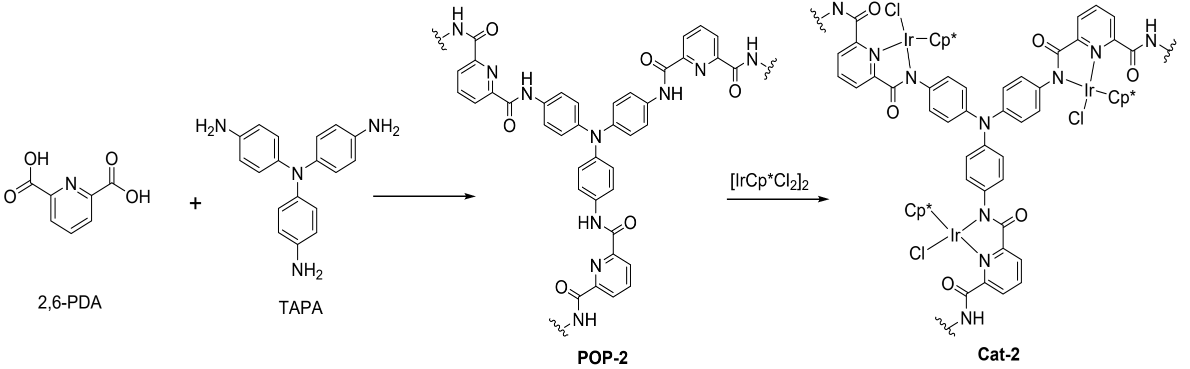

Fig. S2 Synthesis of **POP-2** and **Cat-2**.

2,6-PDA (0.8 mmol, 133.70 mg) was dispersed in anhydrous DMAc (4 mL) to obtain solution A. TAPA (0.4 mmol, 116.14 mg), LiCl (2 mmol, 84.78 mg), TPP (2 mmol, 620.56 mg), Et_3N (2 mmol, 202.38 mg) and DMAc (4 mL) were added into a 25 mL Schlenk flask to obtain solution B. Solution B was degassed and purged with argon (Ar) and heated to 140 °C with continuous stirring at 300 rpm. Then, the solution A was added to solution B. The mixture was maintained 140 °C for 3 days under an Ar atmosphere with continuous stirring at 300 rpm. After the reaction, the contents were allowed to cool naturally. The Ar was stopped and the final opaque solution was poured into methanol. The precipitate was then separated by filtration and washed several times with excess methanol and ultrapure water. The sample was dried under vacuum at 80 °C for 22 h to obtain the final product **POP-2** (145 mg). **POP-2** (40 mg) was dispersed in methanol (5 mL) by sonication. Subsequently, the desired $[Cp^*IrCl_2]_2$ was added to the aforementioned suspension and subjected to sonication for 10 min. After sonication, the mixture was stirred at 65 °C under reflux for 24 h and cooled. The solids were filtered, washed with an excess of methanol and dried under vacuum at 80 °C overnight to obtain catalyst **Cat-2**.

3. Catalytic reactions

All hydrogenation reactions were performed in a 25 mL capacity customized stainless steel reactor equipped with a pressure sensors and gas inlet and outlet ports. In a typical hydrogenation experiment, the reactor was charged with 5 mg of catalyst and 4 mL aqueous solution of base, and then sealed. Before the start of the reaction, the reactor was purged with Ar gas to remove any residual air, and then filled with a mixture of CO_2 and H_2 in a 1:1 ratio, in order to achieve the desired reaction pressure at room temperature. The reactor was heated to the specified temperature while undergoing continuous magnetic stirring at 1000 rpm. After the reaction, the mixture was allowed to cool naturally, and the residual gas was slowly released through a release valve. A liquid sample was collected from the reactor and filtered using a 0.2 μm filter. Finally, the formate concentration was measured using HPLC equipment. In the HPLC analysis, the external standard method was employed for the quantification of the product, which involved the construction of a standard curve. ICP-MS was used to accurately determine the Ir metal content in the synthesized catalysts.

Table S1 Results of the hydrogenation of CO_2 to formate catalyzed by **Cat-1** at different reaction times.

Entry	T (h)	$\text{Conc.}_{\text{formate}}$ (M)	TON
1	0.25	0.030	1025
2	0.5	0.050	1709
3	1	0.15	5126
4	2	0.29	9910
5	4	0.38	12986
6	8	0.49	16744
7	12	0.58	19820
8	24	0.69	23579

Note: Reaction conditions: 5 mg of catalyst (0.45 wt% Ir), 4 mL of water, reaction temperature of 120 °C, reaction pressure of 3 MPa, 2 M K_2CO_3 as base.

Table S2 Results of the hydrogenation of CO_2 to formate catalyzed by **Cat-2** at different reaction times.

Entry	T (h)	Conc.$_{formate}$ (M)	TON
1	0.25	0.09	1922
2	0.5	0.15	3204
3	1	0.33	7048
4	2	0.62	13242
5	4	0.84	17941
6	8	1.07	22853
7	12	1.17	24989
8	24	1.29	27552

Note: Reaction conditions: 5 mg of catalyst (0.72 wt% Ir), 4 mL of water, reaction temperature of 120 °C, reaction pressure of 3 MPa, 2 M K_2CO_3 as base.

Table S3 Results of the hydrogenation of CO_2 to formate catalyzed by **Cat-2** under different H_2 partial pressure.

Entry	H_2 partial Pressure (MPa)	CO_2 partial Pressure (MPa)	$P(H_2)/P(CO_2)$	Conc.$_{formate}$ (M)	TON
1	0	3	0	-	-
2	0.25	2.75	0.091	0.055	1175
3	0.5	2.5	0.2	0.11	2349
4	0.75	2.25	0.33	0.21	4485
5	1	2	0.5	0.39	8330
6	1.25	1.75	0.71	0.62	13242
7	1.5	1.5	1	0.65	13883
8	1.75	1.25	1.4	0.72	15378
9	2	1	2	0.49	10465
10	2.25	0.75	3	0.36	7689
11	2.5	0.5	5	0.27	5767
12	2.75	0.25	11	0.12	2563
13	3	0	-	0.007	150

Note: Reaction conditions: 120 °C, 3 MPa, 5 mg of catalyst (0.72 wt% Ir), 4 mL of water, 2 M K_2CO_3 as base, reaction time 2 h.

4. The elemental composition of porous organic polymers supports

Table S4 Elemental composition of porous organic polymer supports.

sample	N (%)	C (%)	H (%)	C/N ratio	C/H ratio
POP-1	12.08	60.27	4.02	4.9882	14.9800
POP-2	12.41	60.42	4.07	4.8692	14.8397

5. XPS analysis

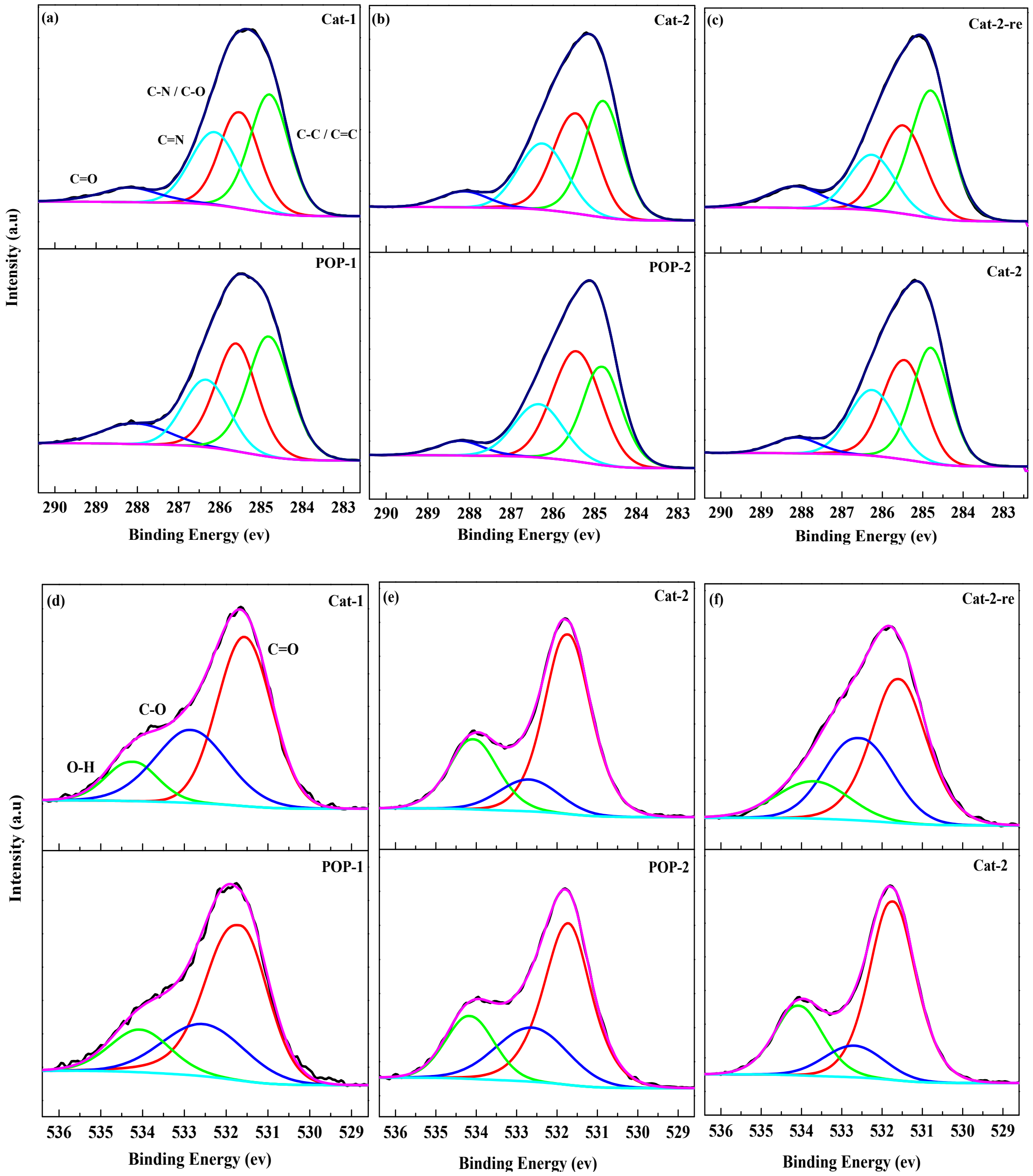

Fig. S3 (a) Deconvoluted C-1s core level XPS spectra of **POP-1** and **Cat-1**.
(b) Deconvoluted C-1s core level XPS spectra of **POP-2** and **Cat-2**.
(c) Deconvoluted C-1s core level XPS spectra of **Cat-2** and **Cat-2-re**.
(d) Deconvoluted O-1s core level XPS spectra of **POP-1** and **Cat-1**.
(e) Deconvoluted O-1s core level XPS spectra of **POP-2** and **Cat-2**.
(f) Deconvoluted O-1s core level XPS spectra of **Cat-2** and **Cat-2-re**.

Table S5 Summary table of binding energy results.

Sample	**POP-1**	**Cat-1**	**POP-2**	**Cat-2**	**Cat-2-re**	complex **4** (R = H)	[Cp*IrCl$_2$]$_2$
Pyridinic-N (eV)	398.58	398.80	398.53	398.79	398.61	398.35	-
C-N (eV)	399.23	399.38	399.16	399.35	399.21	399.91	-
C=O (eV)	531.66	531.56	531.74	531.72	531.57	531.04	-
C-O (eV)	532.54	533.84	532.68	532.69	532.54	532.32	
O-H (eV)	534.06	534.21	534.15	534.06	533.69	532.93	-
Ir 4f$_{5/2}$ (eV)	-	64.64	-	64.66	64.37	64.60	64.95
Ir 4f$_{7/2}$ (eV)	-	61.66	-	61.63	61.44	61.62	61.94
C=C/C-C	284.80	284.80	284.80	284.80	284.80	284.80	
C-N/C-O	285.60	285.51	285.43	285.45	285.49	285.33	
C=N	286.33	286.13	286.33	286.25	286.26	285.96	
C=O	288.04	288.18	288.22	288.13	288.16	287.42	

6. CO_2-TPD profile of Cat-2.

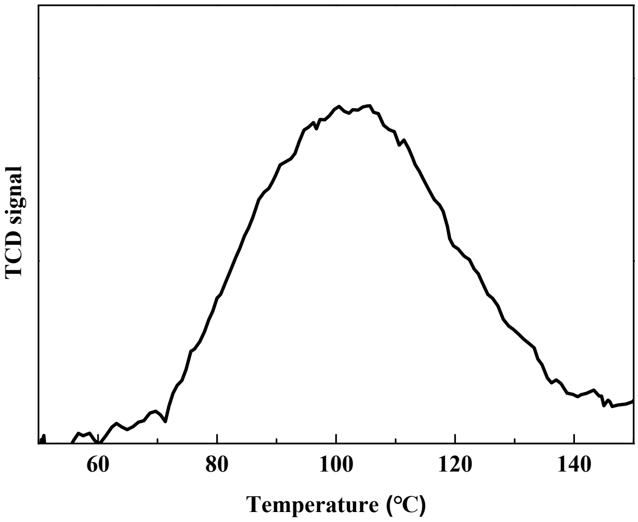

Fig S4. CO_2-TPD profile of **Cat-2**.

7. ^{1}H NMR spectra of the reaction solution

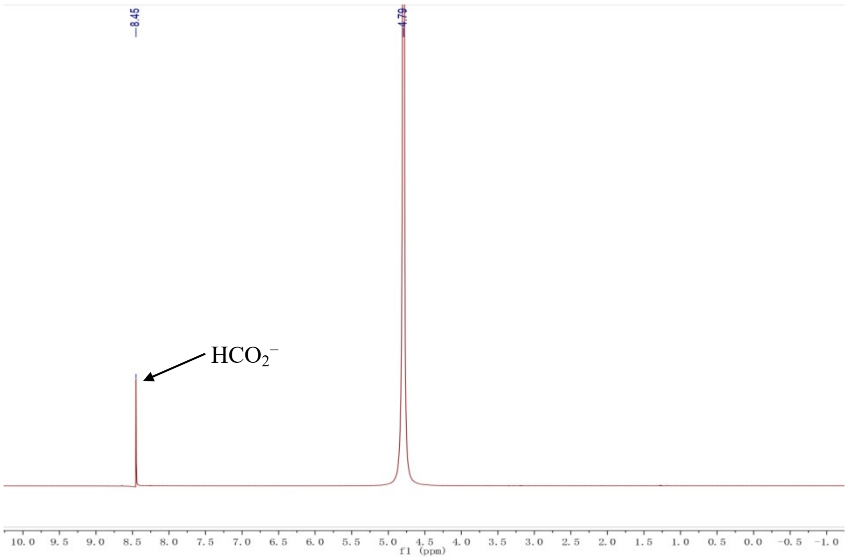

Fig S5. ^{1}H NMR spectra of the solution obtained in Table S2 entry 4 (D_2O).

8. The results of gas chromatography

Table S6 The GC results of the gas mixture obtained from Table S2 entry 4.

t (min)	gas
1.095	air
8.928	CO_2

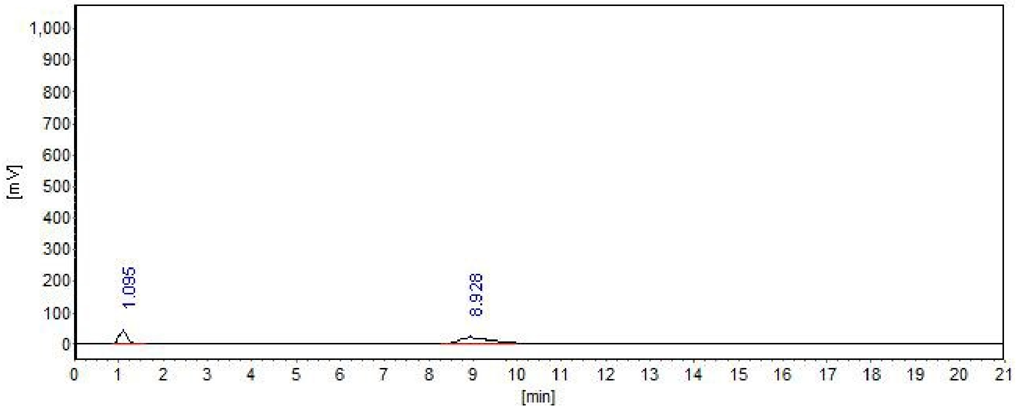

Fig S6. Gas mixture obtained from Table S2 entry 4.

9. Heterogeneity test results of Cat-2

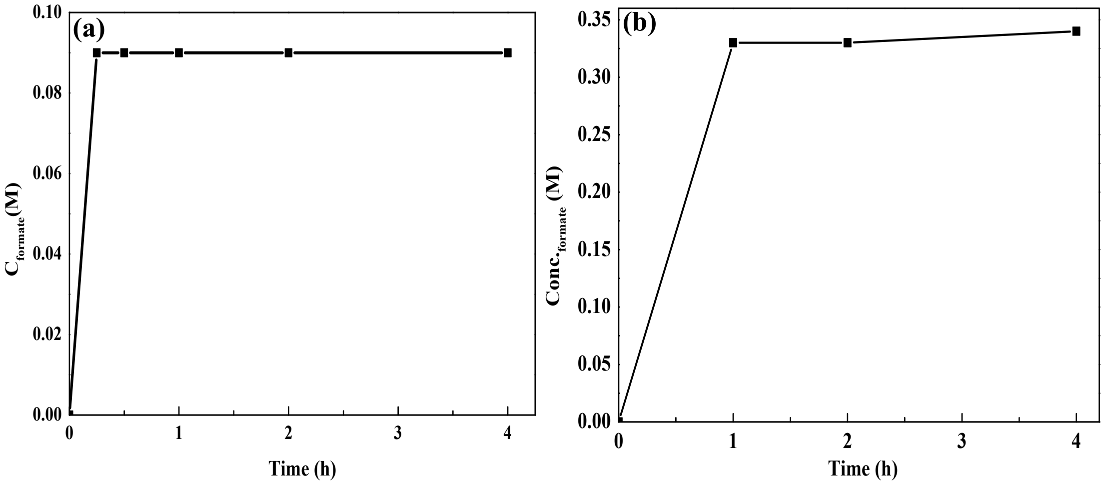

Fig S7. Heterogeneity test results of **Cat-2.**

10. TEM, STEM and EDS mapping

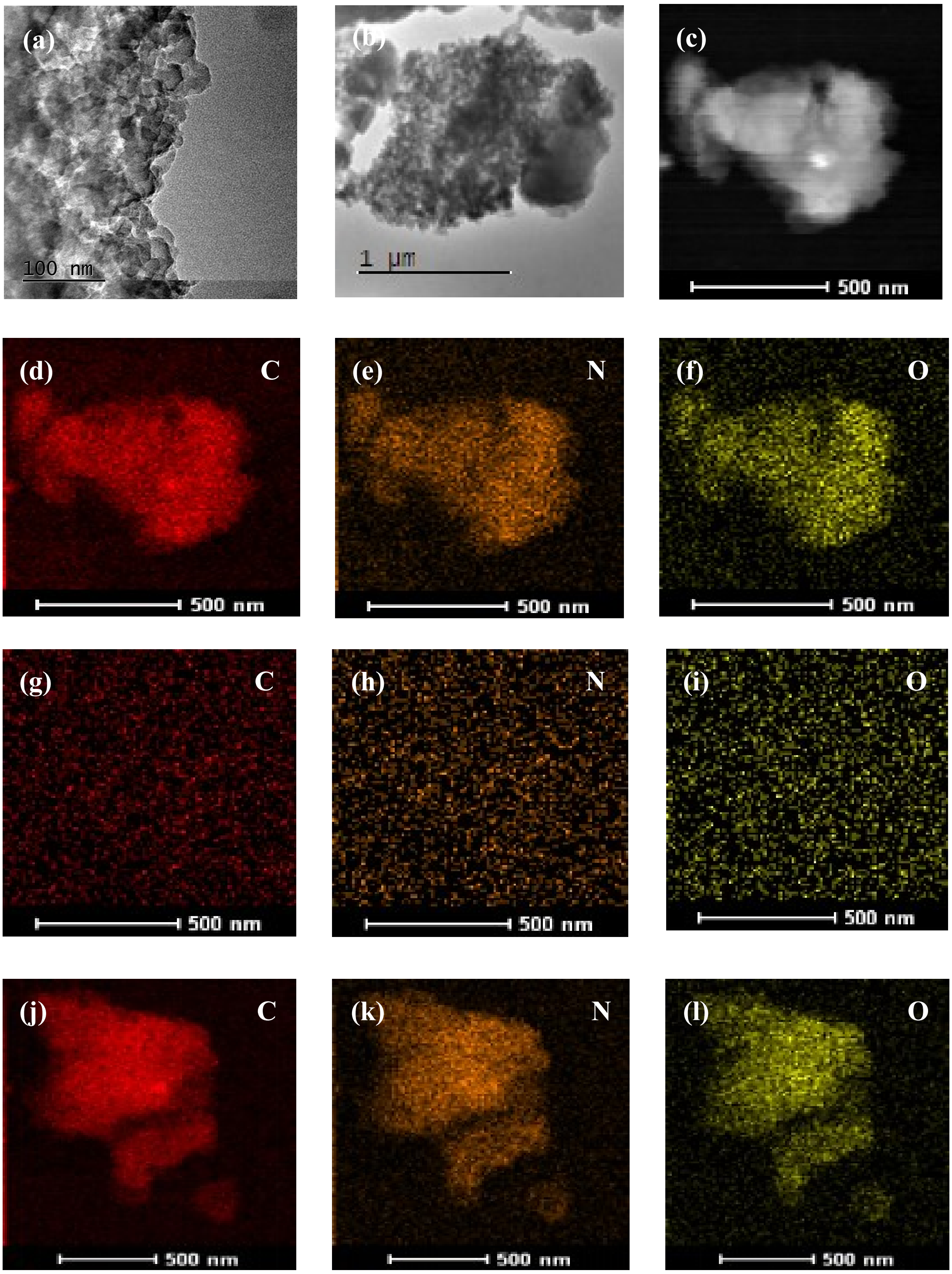

Fig. S8 **POP-2** (a, b) TEM (c) STEM (d-f) EDS elemental mapping.
Original catalyst **Cat-2** (g-i) EDS elemental mapping.
Catalyst **Cat-2-re** (j-l) EDS elemental mapping.

11. Activity comparison of reported heterogeneous catalysts

Table S7 Activity comparison of reported heterogeneous catalysts.

Entry	Catalyst	t (h)	T (°C)	P (MPa) H_2/CO_2 (1/1)	TON	ref
1	bpy-CTF-[IrCp*Cl]Cl	2	120	8	5000	[1]
2	Ir@CTF spheres	2	90	2	358	[2]
3	Ir-NHC-CTFs	15	120	8	24300	[3]
4	$Ir_{1.4}$@bpy-CTF400	2	120	8	5000	[4]
5	$IrCl_3$–phen-POP	2	120	8	14400	[5]
6	Ir-PicaSi-SiO_2	24	150	5	6983	[6]
7	Ru/p-dop-POMs	24	120	8	25400	[7]
8	Ru/N-Me-3-bpp-POP	4	160	4 (1/3)	1877	[8]
9	Ir-HCP-TPM	1	80	5	30891	[9]
10	bpy-PP-POP	24	140	5.6	20041	[10]
11	P-CAAC-Ir	24	100	6 (4/2)	35430	[11]
12	p-PNP-Ir	12	120	7 (5/2)	467300	[12]
13	Ir-PN/SBA-15	20	60	4	2800	[13]
14	Ir@PN-PEI-TNT-Na	20	140	2	1012	[14]
15	Ir-PNP-1	24	150	5	28000	[15]
16	mbpyOH-[IrIII]-UiO	15	85	0.1	6149	[16]
17	Ir@Co_3O_4	6	120	6.2	1955	[17]
18	SBA-15-CAAC-Ir	24	60	6 (4/2)	21050	[18]
19	**Cat -2**	2	120	3	13883	This work
20	**Cat -2**	24	120	3	27552	This work

12. References

[1] K. Park, G. H. Gunasekar , N. Prakash, K. D. Jung, S. Yoon, *ChemSusChem* **2015**, 8, 3410-3413.

[2] A. V. Bavykina, E. Rozhko, M. G. Goesten, T. Wezendonk, B. Seoane, F. Kapteijn, M. Makkee, J. Gascon, *ChemCatChem* **2016**, 8, 2217-2221.

[3] G. H. Gunasekar, K. Park, V. Ganesan, K. Lee, N.-K. Kim, K.-D. Jung, S. Yoon, *Chemistry of Materials* **2017**, 29, 6740-6748.

[4] G. Gunasekar, K. Park, H. Jeong, K.-D. Jung, K. Park, S. Yoon, *Catalysts* **2018**, 8, 295-310.

[5] G. H. Gunasekar, S. Yoon, *Journal of Materials Chemistry A* **2019**, 7, 14019-14026.

[6] L. Tensi, A. V. Yakimov, C. Trotta, C. Domestici, J. De Jesus Silva, S.R. Docherty, C. Zuccaccia, C. Copéret, A. Macchioni, *Inorganic Chemistry* **2022**, 61, 10575-10586.

[7] B. Chen, M. Dong, S. Liu, Z. Xie, J. Yang, S. Li, Y. Wang, J. Du, H. Liu, B. Han, *ACS Catalysis* **2020**, 10, 8557-8566.

[8] H. Park, K. Park, K.-D. Jung, S. Yoon, *Inorganic Chemistry Frontiers* **2021**, 8, 1727-1735.

[9] T. Mandal, A. Kumar, J. Panda, T. Kumar Dutta, J. Choudhury, *Angewandte Chemie International Edition* **2023**, 62, e202314451.

[10] N. R. Bennedsen, D. B. Christensen, R. L. Mortensen, B. Wang, R. Wang, S. Kramer, S. Kegnæs, *ChemCatChem* **2021**, 13, 1781-1786.

[11] L. Zhou, C. Yao, W. Ma, J. Hu, Y. Wu, Z. Zhang, X. Hu, *Journal of CO_2 Utilization* **2021**, 54, 101769.

[12] W. Ma, W. Xiong, J. Hu, J. Geng, X. Hu, *Green Chemistry* **2024**, 26, 4192-4198.

[13] Z. Xu, N. D. McNamara, G. T. Neumann, W. F. Schneider, J. C. Hicks, *ChemCatChem* **2013**, 5, 1769-1771.

[14] Y. Kuwahara, Y. Fujie, H. Yamashita, *ChemCatChem* **2017**, 9, 1906-1914.

[15] H. K. Lo, I. Thiel, C. Copéret, *Chemistry – A European Journal* **2019**, 25, 9443-9446.

[16] B. An, L. Zeng, M. Jia, Z. Li, Z. Lin, Y. Song, Y. Zhou, J. Cheng, C. Wang, W. Lin, *Journal of the American Chemical Society* **2017**, 139, 17747-17750.

[17] B. D. Bankar, K. Ravi, R.J. Tayade, A.V. Biradar, *Journal of CO_2 Utilization* **2023**, 67, 102315.

[18] L. Zhou, L. Peng, X. Hu, *Chinese Journal of Chemical Engineering* **2022**, 50, 283-291.